INFERRING CRUSTAL STRESS-STRAIN ON VENUS USING SHIELD FIELDS: A MATLAB SOFTWARE TOOL. B. J. Thomson[1] and N. P. Lang[2], [1]Boston University Center for Remote Sensing, Boston MA 02215 (bjt@bu.edu), [2]Mercyhurst University, Erie, PA 16546 (nlang@mercyhurst.edu).

Introduction: A consequence of the relative paucity of impact craters on Venus is that the ages of geologic units are largely determined from stratigraphic relationships rather than measuring the number density of impact craters. Yet the task of inferring relative age from stratigraphic relationships is complicated by the >75 m spatial resolution the of the best available radar data from Magellan [1]. One element in finding the stratigraphic position of a given geologic unit is to determine which sets(s) of structures pre-date it. Here, we present a new adaptation of a existing numerical technique to infer the stratigraphic position of clusters of small shield volcanoes, a category of volcanic edifies that are widespread on Venus [2]. An associated abstract [3] presents preliminary results of an application of this model to a venusain shield field.

Background:

Shield field background. Shield fields are clusters of small (1-2 km diameter) shield volcanoes. Each field typically contains tens to hundreds of shields that range in spatial density from 4-10 edifices per 10^3 km^2 within an area of ~10^4 km^2 [2]. Two previous studies of the stratigraphic positions of representative samples of shield fields have reached diametrically opposed results: one found that 42% of shield fields appear to be younger than (i.e., postdate) the regional plains [4], while a different study found that 69% of fields appeared to be older than or predate regional plains [5].

Venus evolutionary models. These contradictory findings are each used as evidence of a particular style of evolutionary model (i.e., directional versus non-directional). These two models are opposing end-members in a fundamental and ongoing debate about the nature of the geologic history of Venus – whether its evolution has progressed in a directional, linear fashion [e.g., 6, 7, 8], or alternatively proceeded in a non-directional manner [e.g., 9-12].

In the directional model, many of the indentified unit types and processes are proposed to have operated synchronously, such as global or near-global emplacement of basalt flood plains (termed "ridged plains") in a catastrophic episode. In contrast, the non-directional model posits that the rate of surface change on Venus has been more steady-state than episodic, and that, for example, different occurrences of ridged plains units may have formed at different times as the epicenter of resurfacing has gradually shifted across the planet.

Numerical method: To quantify preferred orientations in clusters of volcanoes, *Lutz* [13] developed a method known as the two-point azimuth method. In this method, the azimuth or orientation between each feature and all of the other edifices in a population are determined. For N points, there are $N(N–1)/2$ such orientations. The results are binned into a histogram or rose diagram, and peaks in the histogram indicate preferred alignments of features (**Figure 1a-c**). One drawback with this approach is that the overall shape of the distribution of points has a measureable impact on the resulting histogram. A very elongate field with a large aspect ratio (e.g., > 2:1) would exhibit a cluster of preferred orientations consistent with the field shape asymmetry, even if the latter had no controlling influence on the former. Therefore, an attempt is made to determine the statistical significance of the results by comparing the observed distribution to a family of models generated using Monte Carlo techniques with a random distribution of the same number of points in a model space of similar spatial extent [13].

Graphical User Interface (GUI): We have incorporated this algorithm into a graphical user interface (GUI) built with the MATLAB® (MATrix LABoratory) softare. In the GUI, a user selects pre-processed input data, which is a CSV file that contains the center lat, lon position of each edifice in the shield field. The main body of the GUI consists of three panels (**Figure 1d**). In the first panel, the distribution of point features (e.g., shields) can be visually confirmed in a *x*-*y* scatter plot. A second panel displays a raw, uncorrected histogram of orientation measurements. A third panel executes a user-specified number of Monte Carlo runs to randomly place an equivalent number of shields within the boundaries defined by the edge edifices (for fans of linguistics, such a polygon is termed a convex hull). A "normalized" histogram is produced from the Monte Carlo results whereby histogram cell is equal to the expected value times the observed value divided by the mean value in the Monte Carlo runs.

To determine if a given normalized histogram value is statistically significant to the 95% significance level, the Student's t distribution is used to determine the 95th percentile critical threshold value. Histogram values that exceed the critical threshold value are deemed statistically significant.

Results: As a proof-of-concept, a data set from [13] is reproduced in **Figs. 1a-c**. Individual data points are given in Fig. 1a; raw histogram values are given in

Fig. 1b, and normalized histogram values are given in **Fig. 1c**. The three panels in **Fig. 1d** (a snapshot of the GUI) contain, from left to right, a plot of the individual data points, a raw histogram and rose plot, and a normalized histogram. In the normalized histogram, four adjacent 10° bins centered on N60°E exceed the expectations of a random pattern at the 0.05 significance level (as indicated by blue astericks). These results faithfully reproduce the original data in **Figs. 1a-c** and lend confidence the algorithm is executing as designed.

Future work: The prototype GUI is fully functional; preliminary shield field results are given in [3]. A planned modification will account for inputs that are either in decimal degrees (lat, lon) or projected units (*x*-*y* Cartesian coordinates). Future work includes searching for smaller spatial scale anisotropies in the distribution of points to compare with the whole-field results [e.g., 14].

References: [1] Sharpton V.L. (2012) *LPSC*, *43*, #1246. [2] Crumpler L.S. et al. (1997) in *Venus II* 697–756. [3] Lang N.P. & Thomson B.J. (2013) this conference. [4] Addington E.A. (2001) *Icarus*, *149*, 16-36. [5] Ivanov M.A. & Head J.W. (2004) *JGR*, *109*. [6] Schaber G.G. et al. (1992) *JGR*, *97*, 13257-13301. [7] Strom R.G. et al. (1994) *JGR*, *99*, 10,899-810,926. [8] Basilevsky A.T. & Head J.W. (2002) *Geology*, *30*, 1015-1018. [9] Phillips R.J. et al. (1992) *JGR*, *97*, 15,923-915,948. [10] Hauck S.A. et al. (1998) *JGR*, *103*, 13,635-613,642. [11] Guest J.E. & Stofan E.R. (1999) *Icarus*, *139*, 55-66. [12] Romeo I. & Turcotte D.L. (2010) *Planet. Space Sci.*, *58*, 1374-1380. [13] Lutz T.M. (1986) *JGR*, *91*, 421-434. [14] Cebriá J.M. et al. (2011) *JVGR*, *201*, 73-82.

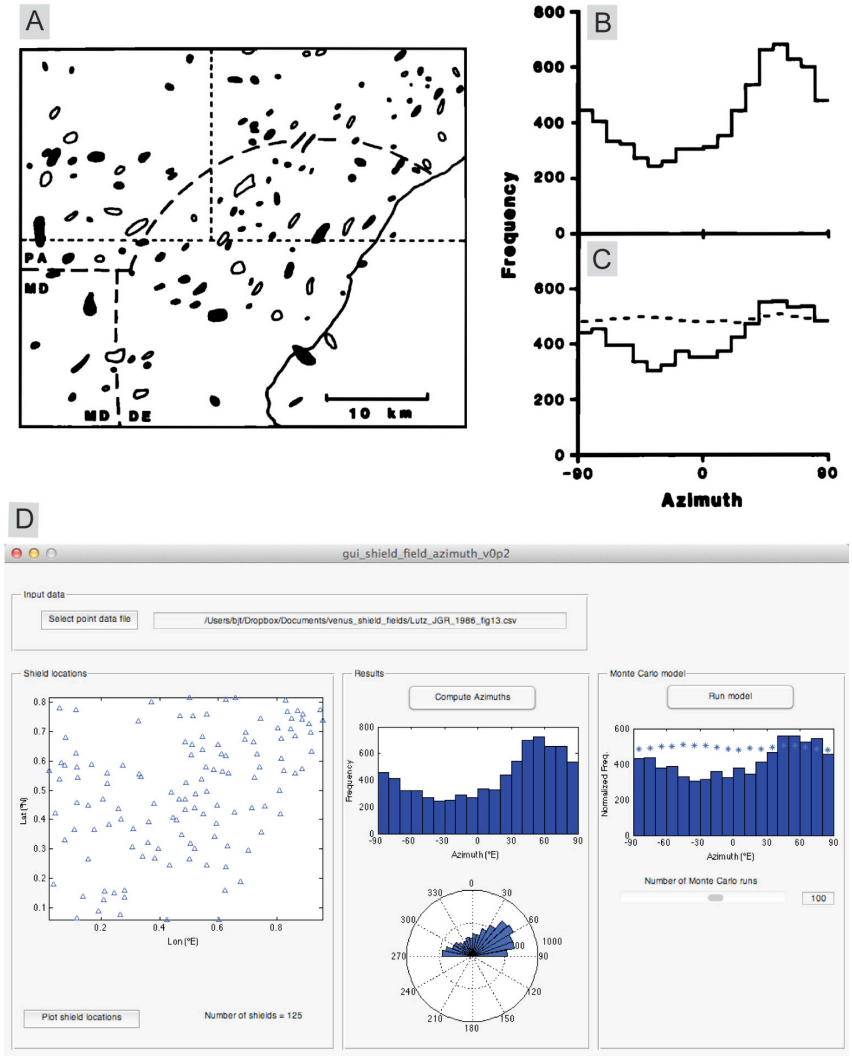

Figure 1. (a) Map of magnetic anomalies in the Pennslyvania, Maryland, and Deleware region [11]. The centroids of the 125 features were used in Figs 1b-d. **(b)** Raw distribution of azimuth values binned into 10° intervals (from [11] Fig. 14a). **(c)** Corrected azimuth distribution; dashed line indicates 95% threshold value (mean+2σ) (from [11] Fig. 14b). **(d)** Snapshot of MATLAB GUI. Ingested data is identical to that in Fig. 1a (with arbitrary lat/lon values); middle and right-hand panels are raw and corrected azimuth histograms, respectively (compare to Fig. 1b-c).